H04

Proceedings of the 5th International Conference on Inverse Problems in Engineering: Theory and Practice, Cambridge, UK, 11-15th July 2005

A SHAPE IDENTIFICATION PROBLEM IN ESTIMATING SIMULTANEOUSLY TWO INTERFACIAL CONFIGURATIONS IN A MULTIPLE REGION DOMAIN

C.-H. Huang and C.-C. Shih
Department of Systems and Naval Mechatronic Engineering, National Cheng Kung University, Tainan, Taiwan 701, R.O.C.
e-mail: chhuang@mail.ncku.edu.tw

Abstract - A two-dimensional shape identification problem, i.e. inverse geometry problem, of estimating simultaneously two interfacial configurations in a multiple (three) region domain is solved in this study by using the Conjugate Gradient Method (CGM) and Boundary Element Method (BEM)-based inverse algorithm. Two over-utilized conditions should be applied in determining two gradient equations, this differs from our previous relevant studies. Numerical experiments using different measurement errors and number of sensors were performed to justify the validity of the conjugate gradient method in solving this shape identification problem. Finally it is concluded that the present algorithm can estimate the accurate interfacial configurations.

1. INTRODUCTION

The objective of the present inverse geometry problem is to estimate the unknown interfacial configurations in a multiple region domain. This approach can be applied to many other applications such as the interface geometry identification for the composite material and for the phase change (Stefan) problems, ice thickness estimation in a thermal storage system and crystal growth estimation, etc. In the previous work by Huang and Chao [3], a steady-state shape identification problem has been solved successfully by using boundary element method with both the Levenberg-Marquardt method (LMM) and conjugate gradient method (CGM) [1]. Based on the algorithm developed in [3], Huang and Tsai [5] extended to a transient inverse geometry problem in identifying the unknown irregular boundary configurations from external measurements. Huang and Chen [2] extended the similar algorithm to a multiple region domain in estimating the time and space varying outer boundary configurations.

Park and Shin applied the coordinate transformation technique with the adjoint variable method to a shape identification problem in determining unknown boundary configurations for heat conduction systems [8] and natural convection systems [9]. It should be noted that except for [2], all the above references are to determine the boundary configurations in a single region domain. In [2], it is a multiple domain problem, but is also in determining the boundary configurations.

Kwag *et al*. [7] followed the algorithm used in [2] to estimate the phase front motion of ice in a thermal storage system. It should be in a multiple region domain, however, the derived sensitivity and adjoint problems become also in a single region domain, i. e. the coupled interfacial conditions are not used to solve those problems. The discussions regarding the determination of interfacial configurations in a multiple region domain has not been reported in the literature.

Recently, Huang and Shih [4] extented the inverse geometry problem based on [2] to a multiple region domain in estimating the unknown interfacial configuration when considering fully expressions of the coupled interfacial conditions for both the sensitivity and adjoint problems. Good estimations for the interfacial configuration were obtained in that study. As we may expect the task of this study is obviously more difficult than [4].

2. THE DIRECT PROBLEM

The following heat conduction problem in a multiple (three) region domain is used to illustrate the methodology for developing expressions in determining simultaneously the interfacial configurations. The boundary conditions for regions Ω_1, Ω_2 and Ω_3 are all assumed insulated at x = 0 and L. The boundary condition for Ω_1 at y = 0 is subjected to a Robin condition with ambient temperature $T_{\infty h}$ and heat transfer coefficient h. The boundary condition for Ω_3 at y = H is also subjected to a Robin condition with ambient temperature $T_{\infty c}$ and heat transfer coefficient h. The interface conditions along $\Gamma_1(x)$ and $\Gamma_2(x)$ are assumed perfect thermal contact condition, i.e. temperatures and heat fluxes for regions Ω_1, Ω_2 and regions Ω_2 , Ω_3 are the same along $\Gamma_1(x)$ and $\Gamma_2(x)$, respectively.

Figure 1 shows the geometry and the coordinates for the composite material considered here, where the dots "●" (M=20) and triangles "Δ" (M=10) denote the sensors' locations on each of the surfaces y = 0 and y = H. The dimensionless mathematical formulation of this heat conduction problem in three regions is given by:

Region Ω_1:

$$\frac{\partial^2 T_1(\Omega_1)}{\partial x^2}+\frac{\partial^2 T_1(\Omega_1)}{\partial y^2}=0 \text{ ; in } \Omega_1 \text{ , and } -k_1\frac{\partial T_1(\Omega_1)}{\partial y}=h(T_{\infty h}-T_1) \text{ ; at } y=0 \qquad (1a,b)$$

$$\frac{\partial T_1(\Omega_1)}{\partial x}=0 \text{ ; at } x=0 \quad \text{and} \quad \frac{\partial T_1(\Omega_1)}{\partial x}=0 \text{ ; at } x=L \qquad (1c,d)$$

Region Ω_2:

$$\frac{\partial^2 T_2(\Omega_2)}{\partial x^2}+\frac{\partial^2 T_2(\Omega_2)}{\partial y^2}=0 \text{ ; in } \Omega_2 \qquad (2a)$$

$$\frac{\partial T_2(\Omega_2)}{\partial x}=0 \text{ ; at } x=0 \quad \text{and} \quad \frac{\partial T_2(\Omega_2)}{\partial x}=0 \text{ ;at } x=L \qquad (2b,c)$$

Region Ω_3:

$$\frac{\partial^2 T_3(\Omega_3)}{\partial x^2}+\frac{\partial^2 T_3(\Omega_3)}{\partial y^2}=0 \text{ ; in } \Omega_3 \quad \text{and} \quad -k_3\frac{\partial T_3(\Omega_3)}{\partial y}=h(T_3-T_{\infty c}) \text{ ; at } y=H \qquad (3a,b)$$

$$\frac{\partial T_3(\Omega_3)}{\partial x}=0 \text{ ;at } x=0 \quad \text{and} \quad \frac{\partial T_3(\Omega_3)}{\partial x}=0 \text{ ; at } x=L \qquad (3c,d)$$

Interfacial conditions for regions Ω_1 and Ω_2:

$$T_1(\Omega_1)=T_2(\Omega_2) \text{ ; } k_1\frac{\partial T_1(\Omega_1)}{\partial y}=k_2\frac{\partial T_2(\Omega_2)}{\partial y} \quad \text{along unknown interface } \Gamma_1(x) \qquad (4a,b)$$

Interfacial conditions for regions Ω_2 and Ω_3:

$$T_2(\Omega_2)=T_3(\Omega_3) \text{ ; } k_2\frac{\partial T_2(\Omega_2)}{\partial y}=k_3\frac{\partial T_3(\Omega_3)}{\partial y} \quad \text{along unknown interface } \Gamma_2(x) \qquad (5a,b)$$

Here subscripts 1, 2 and 3 denote three different regions, respectively; k_1, k_2 and k_3 are the thermal conductivity for regions 1, 2 and 3, respectively. Constant boundary elements over space are adopted for all the examples illustrated here.

3. THE SHAPE IDENTIFICATION PROBLEM

For the shape identification problem, the interfacial configurations along $\Gamma_1(x)$ and $\Gamma_2(x)$ are regarded as being unknown, but everything else in direct problem, i.e. eqns (1) to (5) are known. In addition, temperature readings taken at some appropriate locations at y = 0 and H are considered available.

Referring to Figure 1, we assume that M sensors installed along each y = 0 and H are used to record the temperature information to identify simultaneously the interfacial configurations along $\Gamma_1(x)$ and $\Gamma_2(x)$ in the shape identification calculations. Let the temperature readings taken by these sensors be denoted by $Y_1(x_m,0) \equiv Y_1(x_m)$ and $Y_3(x_m,H) \equiv Y_3(x_m)$; m = 1 to M, where M represents the number of thermocouples. The solution of the present shape identification problem is to be obtained in such a way that the following functional is minimized:

$$\begin{aligned} J\left[\Gamma_1(x),\Gamma_2(x)\right] &= \sum_{m=1}^{M}\{[T_1(x_m)-Y_1(x_m)]^2+[T_3(x_m)-Y_3(x_m)]^2\} \\ &= \sum_{m=1}^{M}\int_{x=0}^{L}\{[T_1(x)-Y_1(x)]^2\delta(x-x_m)+[T_3(x)-Y_3(x)]^2\delta(x-x_m)\}dx \end{aligned} \qquad (6)$$

where $\delta(x-x_m)$ is the Dirac delta function and x_m (m = 1 to M) refers to the measured positions. $T_1(x_m)$ and $T_3(x_m)$ are the estimated or computed temperatures along y = 0 and H at the measurement locations $(x_m,0)$ and (x_m,H), respectively. These quantities are determined from the solution of the direct problem given previously by using the estimated $\Gamma_1(x)$ and $\Gamma_2(x)$ for the exact $\Gamma_1(x)$ and $\Gamma_2(x)$.

4. CONJUGATE GRADIENT METHOD FOR MINIMIZATION

The following iterative process based on the conjugate gradient method [1] can be used for the estimation of unknown interfacial configurations, $\Gamma_1(x)$ and $\Gamma_2(x)$, by minimizing the functional $J[\Gamma_1(x), \Gamma_2(x)]$ as :

$$\Gamma_1^{n+1}(x)=\Gamma_1^{n}(x)-\beta_1^{n}P_1^{n}(x) \quad \text{and} \quad \Gamma_2^{n+1}(x)=\Gamma_2^{n}(x)-\beta_2^{n}P_2^{n}(x) \quad \text{for} \quad n=0,1,2,\cdots\cdots \qquad (7a,b)$$

where β_1^n and β_2^n are the search step sizes, $P_1^n(x)$ and $P_2^n(x)$ are the directions of descent. The definitions of those quantities can be found in [1].

To perform the iterations according to eqn (7), we need to compute the step sizes and the gradients of the functional $J_1'^n(x)$ and $J_2'^n(x)$. In order to develop expressions for the determination of these quantities, the sensitivity problems and adjoint problems are constructed as described below.

4.1 Sensitivity problems and search step sizes

Since the problem involves two unknown interfacial boundary configurations $\Gamma_1(x)$ and $\Gamma_2(x)$, in order to derive the sensitivity problem for each unknown function, we should perturb the unknown function one at a time.

The first sensitivity problem can be obtained from the original direct problem defined by equations (1), (2) and (3) by assuming that when $\Gamma_1(x)$ undergoes a variation $\Delta\Gamma_1(x)$, T_1, T_2 and T_3 are perturbed by $\Delta\hat{T}_1$, $\Delta\hat{T}_2$ and $\Delta\hat{T}_3$, respectively. Then replacing Γ_1 in the direct problem by $\Gamma_1+\Delta\Gamma_1$, T_1 by $T_1+\Delta\hat{T}_1$, T_2 by $T_2+\Delta\hat{T}_2$ and T_3 by $T_3+\Delta\hat{T}_3$, subtracting from the resulting expressions the direct problem and neglecting the second-order terms, the following sensitivity problem for the sensitivity functions $\Delta\hat{T}_1$, $\Delta\hat{T}_2$ and $\Delta\hat{T}_3$ are obtained.

Region Ω_1:

$$\frac{\partial^2\Delta\hat{T}_1(\Omega_1)}{\partial x^2}+\frac{\partial^2\Delta\hat{T}_1(\Omega_1)}{\partial y^2}=0 \text{ ;in } \Omega_1 \quad \text{and} \quad -k_1\frac{\partial\Delta\hat{T}_1(\Omega_1)}{\partial y}=-h\Delta\hat{T}_1 \text{ ; at } y=0 \qquad (8a,b)$$

$$\frac{\partial\Delta\hat{T}_1(\Omega_1)}{\partial x}=0 \text{ ;at } x=0 \quad \text{and} \quad \frac{\partial\Delta\hat{T}_1(\Omega_1)}{\partial x}=0 \text{ ; at } x=L \qquad (8c,d)$$

Region Ω_2:

$$\frac{\partial^2\Delta\hat{T}_2(\Omega_2)}{\partial x^2}+\frac{\partial^2\Delta\hat{T}_2(\Omega_2)}{\partial y^2}=0 \quad ; \qquad \text{in } \Omega_2 \qquad (9a)$$

$$\frac{\partial\Delta\hat{T}_2(\Omega_2)}{\partial x}=0 \text{ ; at } x=0 \quad \text{and} \quad \frac{\partial\Delta\hat{T}_2(\Omega_2)}{\partial x}=0 \text{ ; at } x=L \qquad (9b,c)$$

Region Ω_3:

$$\frac{\partial^2\Delta\hat{T}_3(\Omega_3)}{\partial x^2}+\frac{\partial^2\Delta\hat{T}_3(\Omega_3)}{\partial y^2}=0 \text{ ;in } \Omega_3 \quad \text{and} \quad -k_3\frac{\partial\Delta\hat{T}_3(\Omega_3)}{\partial y}=h\Delta\hat{T}_3 \text{ ; at } y=H \qquad (10a,b)$$

$$\frac{\partial\Delta\hat{T}_3(\Omega_3)}{\partial x}=0 \text{ ; at } x=0 \quad \text{and} \quad \frac{\partial\Delta\hat{T}_3(\Omega_3)}{\partial x}=0 \text{ ; at } x=L \qquad (10c,d)$$

Interfacial conditions for regions Ω_1 and Ω_2:

$$\Delta\hat{T}_1(\Omega_1)=T_1(\Omega_1;\Gamma_1+\Delta\Gamma_1,\Gamma_2)-T_1(\Omega_1;\Gamma_1,\Gamma_2)\cong\Delta\Gamma_1\frac{\partial T_1}{\partial y} \quad \text{; along } \Gamma_1(x) \qquad (11a)$$

$$\Delta\hat{T}_2(\Omega_2)=T_2(\Omega_2;\Gamma_1+\Delta\Gamma_1,\Gamma_2)-T_2(\Omega_1;\Gamma_1,\Gamma_2)\cong\Delta\Gamma_1\frac{\partial T_2}{\partial y} \quad \text{; along } \Gamma_1(x) \qquad (11b)$$

Interfacial conditions for regions Ω_2 and Ω_3:

$$\Delta\hat{T}_2(\Omega_2)=\Delta\hat{T}_3(\Omega_3)\text{ ; }k_2\frac{\partial\Delta\hat{T}_2(\Omega_2)}{\partial y}=k_3\frac{\partial\Delta\hat{T}_3(\Omega_3)}{\partial y} \quad \text{along unknown interface } \Gamma_2(x) \qquad (12a,b)$$

We should note that the sensitivity problems are now de-coupled as two independent problems at $y=\Gamma_1(x)$ since the interface conditions along $\Gamma_1(x)$ become independent to each other.

Based on eqns (4) and (11), the following interfacial conditions can also be obtained

$$k_1\Delta\hat{T}_1(\Omega_1)=k_2\Delta\hat{T}_2(\Omega_2)\text{ ; }k_1\frac{\partial\Delta\hat{T}_1(\Omega_1)}{\partial y}=k_2\frac{\partial\Delta\hat{T}_2(\Omega_2)}{\partial y} \quad \text{along } \Gamma_1(x) \qquad (13a,b)$$

The above two equations are needed in deriving the interfacial conditions for adjoint problems.

Similarly, the second sensitivity problem can be obtained by assuming that when $\Gamma_2(x)$ undergoes a variation $\Delta\Gamma_2(x)$, T_1, T_2 and T_3 is perturbed by $\Delta\tilde{T}_1$, $\Delta\tilde{T}_2$ and $\Delta\tilde{T}_3$, respectively. By following the same procedures as stated before, the equations for the second sensitivity problem are identical to the first sensitivity

problem except for the interfacial conditions. The interfacial conditions for the second sensitivity problem can be obtained as

Interfacial conditions for regions Ω_1 and Ω_2:

$$\Delta\tilde{T}_1(\Omega_1) = \Delta\tilde{T}_2(\Omega_2) \quad \text{and} \quad k_1 \frac{\partial \Delta\tilde{T}_1(\Omega_1)}{\partial y} = k_2 \frac{\partial \Delta\tilde{T}_2(\Omega_2)}{\partial y} \quad \text{along } \Gamma_1(x) \tag{14a,b}$$

Interfacial conditions for regions Ω_2 and Ω_3:

$$\Delta\tilde{T}_2(\Omega_2) = T_2(\Omega_2;\Gamma_1,\Gamma_2+\Delta\Gamma_2) - T_2(\Omega_2;\Gamma_1,\Gamma_2) \cong \Delta\Gamma_2 \frac{\partial T_2}{\partial y} \text{ ; along } \Gamma_2(x) \tag{15a}$$

$$\Delta\tilde{T}_3(\Omega_3) = T_3(\Omega_3;\Gamma_1,\Gamma_2+\Delta\Gamma_2) - T_3(\Omega_2;\Gamma_1,\Gamma_2) \cong \Delta\Gamma_2 \frac{\partial T_3}{\partial y} \text{ ; along } \Gamma_2(x) \tag{15b}$$

Based on eqns (5) and (15), the following interfacial conditions along $\Gamma_2(x)$ can also be obtained

$$k_2\Delta\tilde{T}_2(\Omega_2) = k_3\Delta\tilde{T}_3(\Omega_3) \quad ; \quad k_2 \frac{\partial \Delta\tilde{T}_2(\Omega_2)}{\partial y} = k_3 \frac{\partial \Delta\tilde{T}_3(\Omega_3)}{\partial y} \quad \text{along } \Gamma_2(x) \tag{16a,b}$$

Equations (16a) and (16b) are needed in deriving the interfacial conditions for adjoint problems. The search step sizes are determined by minimizing the functional (6) with respect to β_1^n and β_2^n, respectively. The following expressions are obtained for the determination of search step sizes.

$$\beta_1^n = \frac{\sum_{m=1}^{M} \int_{x=0}^{L} [T_1(x) - Y_1(x)]\Delta\hat{T}_1(x)\delta(x-x_m)dx}{\sum_{m=1}^{M} \int_{x=0}^{L} \Delta\hat{T}_1^2(x)\delta(x-x_m)dx} \quad \text{and} \quad \beta_2^n = \frac{\sum_{m=1}^{M} \int_{x=0}^{L} [T_3(x) - Y_3(x)]\Delta\tilde{T}_3(x)\delta(x-x_m)dx}{\sum_{m=1}^{M} \int_{x=0}^{L} \Delta\tilde{T}_3^2(x)\delta(x-x_m)dx} \tag{17a,b}$$

4.2 Adjoint problem and gradient equation

To obtain the first adjoint problem, eqns (1a), (2a) and (3a) are multiplied by the Lagrange multipliers (or adjoint functions) $\lambda_1(\Omega_1)$, $\lambda_2(\Omega_2)$ and $\lambda_3(\Omega_3)$, respectively, and the resulting expression is integrated over the corresponding space domains. Then the result is added to the right hand side of eqn (6). By following the similar procedure as was discussed in [1], the following adjoint problems for the determination of $\lambda_1(\Omega_1)$, $\lambda_2(\Omega_2)$ and $\lambda_3(\Omega_3)$ are obtained

Region Ω_1:

$$\frac{\partial^2\lambda_1(\Omega_1)}{\partial x^2} + \frac{\partial^2\lambda_1(\Omega_1)}{\partial y^2} = 0 \text{ ; in } \Omega_1 \quad \text{and} \quad -\frac{\partial\lambda_1(\Omega_1)}{\partial y} = -\frac{h}{k_1}\lambda_1 + \sum_{m=1}^{M} 2[T_1 - Y_1]\delta(x-x_m) \text{ ; at } y = 0 \tag{18a,b}$$

$$\frac{\partial\lambda_1(\Omega_1)}{\partial x} = 0 \text{ ; at } x = 0 \quad \text{and} \quad \frac{\partial\lambda_1(\Omega_1)}{\partial x} = 0 \text{ ; at } x = L \tag{18c,d}$$

Region Ω_2:

$$\frac{\partial^2\lambda_2(\Omega_2)}{\partial x^2} + \frac{\partial^2\lambda_2(\Omega_2)}{\partial y^2} = 0 \text{ ; in } \Omega_2 \tag{19a}$$

$$\frac{\partial\lambda_2(\Omega_2)}{\partial x} = 0 \text{ ; at } x = 0 \quad \text{and} \quad \frac{\partial\lambda_2(\Omega_2)}{\partial x} = 0 \text{ ; at } x = L \tag{19b,c}$$

Region Ω_3:

$$\frac{\partial^2\lambda_3(\Omega_3)}{\partial x^2} + \frac{\partial^2\lambda_3(\Omega_3)}{\partial y^2} = 0 \text{ ; in } \Omega_2 \quad \text{and} \quad \frac{\partial\lambda_3(\Omega_3)}{\partial y} = -\frac{h}{k_3}\lambda_3 + \sum_{m=1}^{M} 2[T_3 - Y_3]\delta(x-x_m) \text{ ; at } y = H \tag{20a,b}$$

$$\frac{\partial\lambda_3(\Omega_3)}{\partial x} = 0 \text{ ; at } x = 0 \quad \text{and} \quad \frac{\partial\lambda_3(\Omega_3)}{\partial x} = 0 \text{ ; at } x = L \tag{20c,d}$$

Interfacial conditions for regions Ω_1 and Ω_2:

$$k_2\lambda_1(\Omega_1) = k_1\lambda_2(\Omega_2) \quad \text{and} \quad k_2 \frac{\partial\lambda_1(\Omega_1)}{\partial y} = k_1 \frac{\partial\lambda_2(\Omega_2)}{\partial y} \quad ; \quad \text{along } \Gamma_1(x) \tag{21a,b}$$

Interfacial conditions for regions Ω_2 and Ω_3:

$$k_3\lambda_2(\Omega_2) = k_2\lambda_3(\Omega_3) \quad \text{and} \quad \frac{\partial\lambda_2(\Omega_2)}{\partial y} = \frac{\partial\lambda_3(\Omega_3)}{\partial y} \quad ; \quad \text{along } \Gamma_2(x) \tag{22a,b}$$

The standard techniques of BEM can be used to solve the above adjoint problems.

Finally the gradients of functional $J_1'(x)$ and $J_2'(x)$ can be obtained as:

$$J_1'(x) = -\frac{\partial T_1}{\partial y}\frac{\partial \lambda_1}{\partial y}\Big|_{y=\Gamma_1} \quad \text{and} \quad J_2'(x) = \frac{\partial T_3}{\partial y}\frac{\partial \lambda_3}{\partial y}\Big|_{y=\Gamma_2} \qquad (23a,b)$$

5. RESULTS AND DISCUSSIONS

To illustrate the validity of the present inverse algorithms in identifying interfacial boundary configurations $\Gamma_1(x)$ and $\Gamma_2(x)$ simultaneously in a multiple region domain from the knowledge of temperature recordings, we consider three specific examples for the following numerical experiments.

The objective of this study is to show the accuracy of the present algorithm in simultaneously estimating interfacial configurations $\Gamma_1(x)$ and $\Gamma_2(x)$ with no prior information on the functional form of the unknown quantities, which is the so-called function estimation. Moreover, it can be shown numerically that the number of sensor can be reduced when the conjugate gradient method is applied.

In order to compare the results for situations when random measurement errors are considered, we assume normally distributed uncorrelated errors with zero mean and constant standard deviation. The simulated inexact measurement data $\mathbf{Y}_1$ and $\mathbf{Y}_3$ can be expressed as

$$\mathbf{Y}_1 = \mathbf{Y}_{1,\text{exact}} + \omega\,\sigma_1 \quad \text{and} \quad \mathbf{Y}_3 = \mathbf{Y}_{3,\text{exact}} + \omega\,\sigma_3 \qquad (24a,b)$$

where $\mathbf{Y}_{1,\text{exact}}$ and $\mathbf{Y}_{3,\text{exact}}$ are the solutions of the direct problem with the exact $\Gamma_1(x)$ and $\Gamma_2(x)$; σ_1 and σ_3 are the standard deviation of the measurements; and ω is a random variable that generated by subroutine DRNNOR of the IMSL [6] and will be within -2.576 to 2.576 for the 99% confidence bounds. The stopping criterion ε is calculated based on the discrepancy principle [1].

In all the test cases considered here we have chosen L = 10.0 m, H = 3.0 m, $T_{\infty h}$ = 100 ^oC, $T_{\infty c}$ = 10 ^oC and h = 10 W/m^2-^{o}C. Twenty constant elements are used on both upper and lower boundaries, while twenty constant elements are also adopted for each domain on the right and left boundaries. The sensor's locations are placed along y = 0 and H m, i.e. on the lower and upper boundaries. The initial guess for all test case considered here is chosen as $\Gamma_1^0(x)$ = 1.0 m and $\Gamma_2^0(x)$ = 2.0 m.

We now present below the numerical experiments in simultaneously determining $\Gamma_1(x)$ and $\Gamma_2(x)$ by the present shape identification analysis. The unknown boundary configurations at y = $\Gamma_1(x)$ and $\Gamma_2(x)$ are assumed to vary with x in the form

$$\Gamma_1(x) = \begin{cases} 0.7 + 0.12x\ ; & 0 \le x \le \dfrac{L}{2} \\ 1.9 - 0.12x\ ; & \dfrac{L}{2} < x \le L \end{cases} \quad \text{and} \quad \Gamma_2(x) = 2.0 + 0.3\sin\left(\frac{\pi x}{5}\right)\ ;\quad 0 \le x \le L \qquad (25a,b)$$

Firstly the shape identification analysis is performed by assuming k_1 = 3, k_2 = 20, and k_3 = 8 W/m-^{o}C. Twenty thermocouple measurements are used, i.e. M = 20, along y = 0 and H m (referring to Figure 1 where the solid circular dots denote the sensors' location) with thermocouple spacing Δx = 0.5 m. The estimated results for the interfacial configurations of $\Gamma_1(x)$ and $\Gamma_2(x)$ by using measurement errors (σ_1, σ_3) = (0.0,0.0), (0.4,0.1) and (0.8,0.2) are reported in Table 1. The average relative errors between exact and estimated interfacial boundary configurations are defined as

$$\text{ERR1} = \sum_{m=0}^{M}\left|\frac{\Gamma_1(x_m) - \hat{\Gamma}_1(x_m)}{\Gamma_1(x_m)}\right| \div [M+1] \times 100\% \quad \text{and} \quad \text{ERR2} = \sum_{m=0}^{M}\left|\frac{\Gamma_2(x_m) - \hat{\Gamma}_2(x_m)}{\Gamma_2(x_m)}\right| \div [M+1] \times 100\% \qquad (26a,b)$$

Here (M+1) represents the total discrete number of unknown parameters, while Γ_1, Γ_2 and $\hat{\Gamma}_1, \hat{\Gamma}_2$ denote the exact and estimated values of interfacial configurations.

When examining the result of estimations in Table 1, we have (ERR1,ERR2) = (1.20 % ,0.91 %) for (σ_1, σ_3) = (0.0,0.0). This implies that good estimation for $\Gamma_1(x)$ and $\Gamma_2(x)$ have been obtained since very accurate interfacial shapes can be estimated. When the case (σ_1, σ_3) = (0.8,0.2) is considered, the estimated results reveal that (ERR1,ERR2) = (5.52%,8.16%) is obtained. Here (σ_1, σ_3) = (0.8,0.2) represents about 1.0 % of the average measured temperature since the average measured temperatures on y = 0 and H are about 80 and 20, respectively.

This implies that the measurement error needs to be a very small number to obtain a reliable solution. This is reasonable because when k_1=k_2=k_3, i.e. homogeneous material, it is impossible to estimate the shape of interfacial boundaries since the measured temperatures along y = 0 and H will always be the same for different interfacial geometry. For this reason we expect that as the value of difference between k_1, k_2 and k_3 is increased, good estimations should be obtained by using less accurate measurement data.

The analysis is then proceeding to the case when the values of difference between k_1, k_2 and k_3 are increased. Here k_1 = 3, k_2 = 100 and k_3 = 8 W/m-^{o}C and using 20 thermocouple measurements, i.e. M = 20, along y = 0 and H are assumed. When using (σ_1, σ_3) = (0.0,0.0) and ε = 0.006, after 13 iterations the interfacial shapes can be obtained and is plotted in Figure 2 and reported in Table 1. The average relative errors for this case are calculated as (ERR1,ERR2) = (0.60%,0.55%) and is about of the same order when comparing with the previous test case with exact measurements in Table 1.

Next let us discuss the influence of the measurement errors on the inverse solutions. First, the measurement errors for the temperature are taken as (σ_1, σ_3) = (0.8,0.2), i.e. about 1 % of the average measured temperature. Then error is increased to (σ_1, σ_3) = (1.6,0.4), i.e. about 2 % of the average measured temperature. The estimated interfacial shapes for (σ_1, σ_3) = (0.8,0.2) are shown in Figures 3, which are also reported in Table 1.

The number of iteration for (σ_1, σ_3) = (0.8,0.2) is 2 and the average errors for $\Gamma_1(x)$ and $\Gamma_2(x)$ are calculated as (ERR1,ERR2) = (3.41%,5.21%). The number of iteration for (σ_1, σ_3) = (0.8,0.2) is also 2 and the average errors for $\Gamma_1(x)$ and $\Gamma_2(x)$ are calculated as (ERR1,ERR2) = (3.42%,5.26%). By comparing the estimated results of the above cases in Table 1 we found what we expected that when the value of difference between k_1, k_2 and k_3 is increased, good estimations can be obtained by using less accurate measurement data.

Can the number of sensors be reduced with the present approaches? In the CGM, the measurement temperatures at sensors' locations represent the boundary point sources that appeared in the adjoint equations (18b) and (20b). It is possible to reduce the number of boundary point sources even though it will influence the values of J_1' and J_2'. Now the question is how this strategy will influence the accuracy of the inverse solutions? To answer this, the numerical experiments are moved on to the case with M = 10 (Δx = 1.0 m) in simultaneous estimating $\Gamma_1(x)$ and $\Gamma_2(x)$ with measurement errors (σ_1, σ_3) = (0.0,0.0) and (0.8,0.2), respectively. The estimated interfacial configurations are plotted in Figures 2 and 3, respectively, and the results are also reported in Table 1 as well.

From the above comparisons of figures and numerical data we learned that the inverse solutions in predicting $\Gamma_1(x)$ and $\Gamma_2(x)$ with 20 sensors are slightly better than that with 10 sensors; however, the latter case is already good enough to be accepted as the inverse solutions. This represents that the number of sensors can be reduced when the CGM is applied.

Besides, when using (σ_1, σ_3) = (1.6,0.4) and M = 20, it represents about 2 % measurement error. When using this 2 % error, the resultant average errors for $\Gamma_1(x)$ and $\Gamma_2(x)$ are obtained as (ERR1,ERR2) = (3.42%,5.26%). This implies that the CGM is not sensitive to the measurement errors since the measurement errors did not amplify the errors of the estimated boundary shapes (the errors are of the same order). Therefore this technique provides confidence estimation.

6. CONCLUSIONS

The conjugate gradient method (CGM) was successfully applied for the solution of the shape identification problem to determine simultaneously the unknown irregular interfacial configurations by utilizing temperature readings. Several test cases involving different functional forms of $\Gamma_1(x)$ and $\Gamma_2(x)$, different measurement errors and different number of sensors were considered. The results show that (1). The CGM needs very short CPU time on Pentium IV 1.4 GHz PC; (2). The CGM is not sensitive to the measurement errors and (3). The number of sensors can be reduced in performing the shape identification calculations.

Acknowledgment

This work was supported in part through the National Science Council, R. O. C., Grant number, NSC-93-2611-E-006-015.

REFERENCES

1. O.M. Alifanov, *Inverse Heat Transfer Problems*, Springer-Verlag, Berlin Heidelberg, 1994.
2. C.H. Huang and H.M. Chen, An inverse geometry problem of identifying growth of boundary shapes in a multiple region domain. *Numerical Heat Transfer; Part A* (1999) **35**, 435-450.
3. C.H. Huang and B.H. Chao, An inverse geometry problem in identifying irregular boundary configurations. *Int. J. Heat Mass Transfer* (1997) **40**, 2045-2053.
4. C.H. Huang and C.C. Shih, A shape identification problem in estimating the interfacial configurations in a multiple region domain. *J. Thermophys Heat Transfer*, 2004 (accepted).
5. C.H. Huang and C.C. Tsai, A transient inverse two-dimensional geometry problem in estimating time-dependent irregular boundary configurations. *Int. J. Heat Mass Transfer* (1998) **41**, 1707-1718.
6. IMSL Library Edition 10.0. User's Manual: Math Library Version 1.0, IMSL. Houston, TX, 1987.
7. D.S. Kwag, I.S. Park and W.S. Kim, Inverse geometry problem of estimating the phase front motion of ice in a thermal storage system. *Inverse Problems in Engineering* (2004) **12**, 1-15.

8. H.M. Park and H.J. Shin, Empirical reduction of modes for the shape identification problems of heat conduction systems. *Comput. Meth. Appl. Mech. Eng.* (2003) **192**, 1893-1908.
9. H.M. Park and H.J. Shin, Shape identification for natural convection problems using the adjoint variable method. *J. Comput. Phys.* (2003) **186**, 198-211.

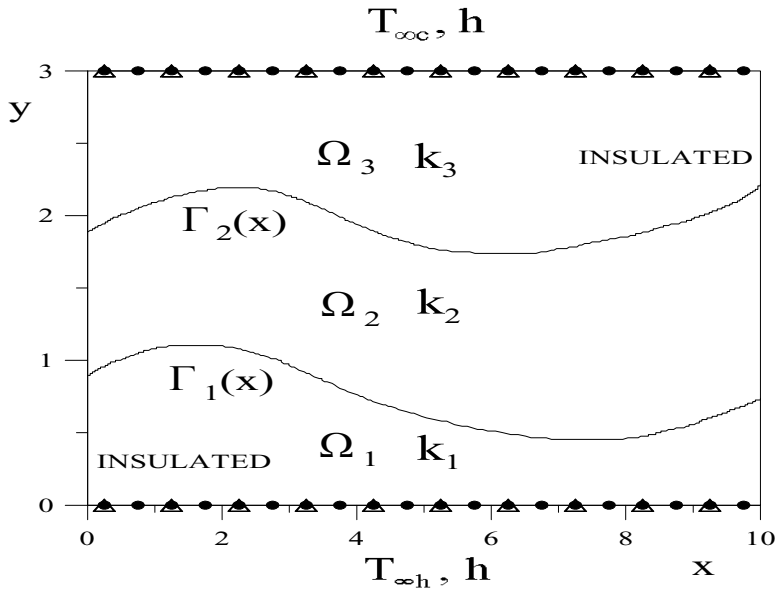

Figure 1. Geometry and coordinates.

Given Conditions \ Estimated Results		Convergence criterion, ε	Number of iteration	Average errors, %,
$k_1 = 3$, $k_2 = 20$, $k_3 = 8$; $(\sigma_1,\sigma_3) = (0.0,0.0)$	M=20	0.006	37	ERR1 = 1.20 %
				ERR2 = 0.91 %
	M=10	0.006	78	ERR1 = 2.41 %
				ERR2 = 2.84 %
$k_1 = 3$, $k_2 = 20$, $k_3 = 8$; $(\sigma_1,\sigma_3) = (0.4,0.1)$	M=20	3.4	2	ERR1 = 5.47 %
				ERR2 = 8.15 %
	M=10	1.7	3	ERR1 = 6.59 %
				ERR2 = 8.00 %
$k_1 = 3$, $k_2 = 20$, $k_3 = 8$; $(\sigma_1,\sigma_3) = (0.8,0.2)$	M=20	13.6	2	ERR1 = 5.52 %
				ERR2 = 8.16 %
	M=10	6.8	2	ERR1 = 10.88 %
				ERR2 = 8.69 %
$k_1 = 3$, $k_2 = 100$, $k_3 = 8$; $(\sigma_1,\sigma_3) = (0.0,0.0)$	M=20	0.006	13	ERR1 = 0.60 %
				ERR2 = 0.55 %
	M=10	0.006	19	ERR1 = 2.04 %
				ERR2 = 1.28 %
$k_1 = 3$, $k_2 = 100$, $k_3 = 8$; $(\sigma_1,\sigma_3) = (0.4,0.1)$	M=20	3.4	3	ERR1 = 2.73 %
				ERR2 = 2.93 %
	M=10	1.7	5	ERR1 = 4.71 %
				ERR2 = 3.40 %
$k_1 = 3$, $k_2 = 100$, $k_3 = 8$; $(\sigma_1,\sigma_3) = (0.8,0.2)$	M=20	13.6	2	ERR1 = 3.41 %
				ERR2 = 5.21 %
	M=10	6.8	3	ERR1 = 5.70 %
				ERR2 = 5.35 %
$k_1 = 3$, $k_2 = 100$, $k_3 = 8$; $(\sigma_1,\sigma_3) = (1.6,0.4)$	M=20	54.4	2	ERR1 = 3.42 %
				ERR2 = 5.26 %
	M=10	27.2	2	ERR1 = 8.10 %
				ERR2 = 6.95 %

Table 1. The estimated parameters for numerical tests.

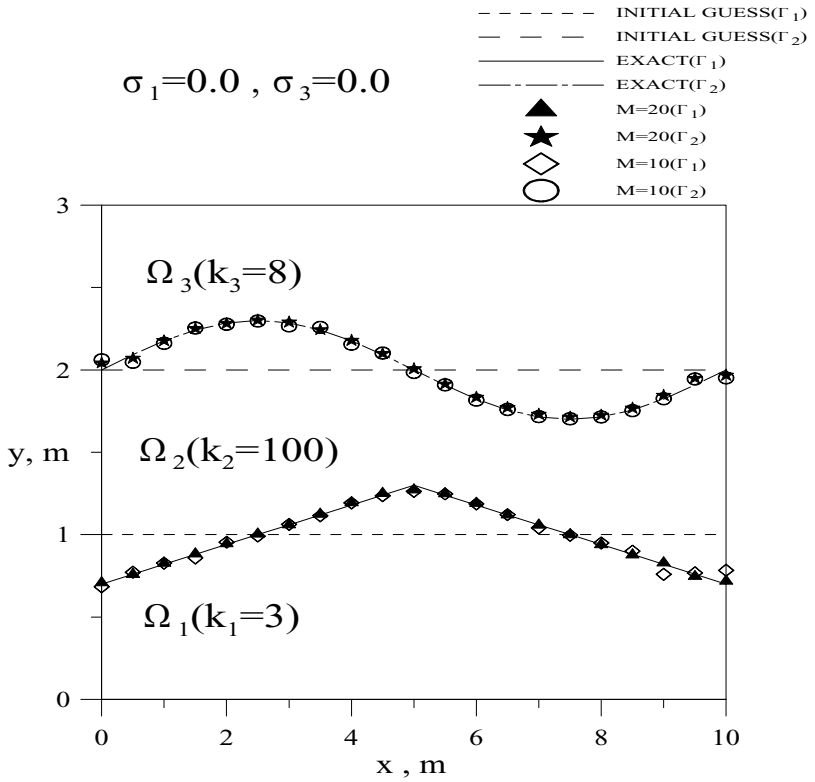

Figure 2. Exact and Estimated Interfacial Configurations by using $(\sigma_1,\sigma_3) = (0.0,0.0)$.

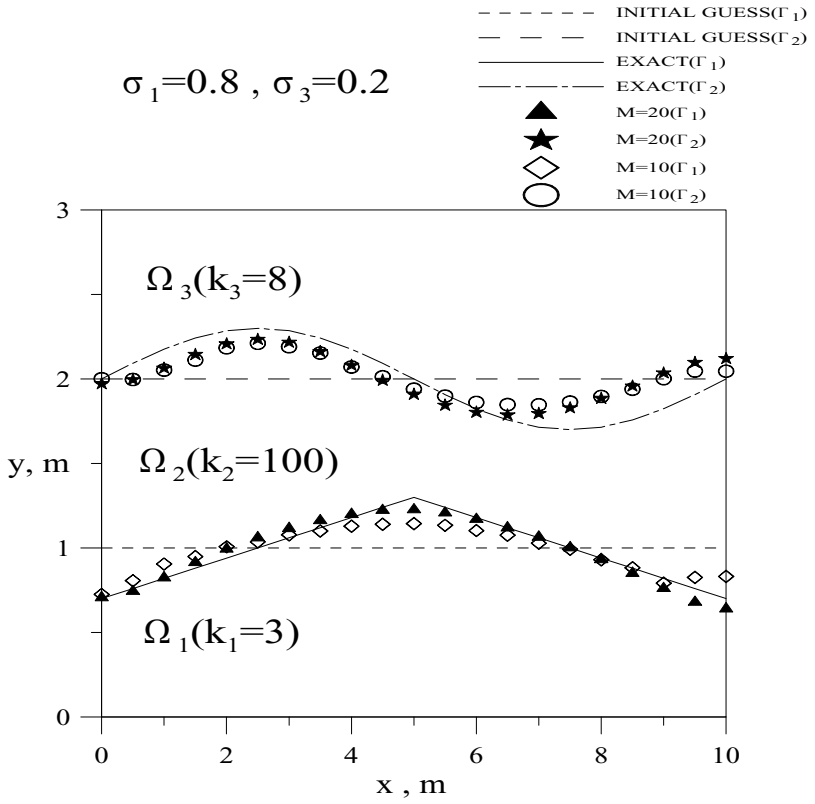

Figure 3. Exact and Estimated Interfacial Configurations by using $(\sigma_1,\sigma_3) = (0.8,0.2)$.